Breast Cancer Classification Using GLCM and BPNN

Syam Julio A. Sarosa[1], Fitri Utaminingrum[2], Fitra A. Bachtiar[3]

[1,2]Computer Vision Research Group, Faculty of Computer Science, Brawijaya University, Malang, Indonesia
[3]Intelligent Systems Research Group, Faculty of Computer Science, Brawijaya University, Malang, Indonesia
e-mail: syamjulio@gmail.com, f3_ningrum@ub.ac.id, fitra.bachtiar@ub.ac.id

Abstract

Among all the cancer in women, breast cancer is the most common and deadliest cancer. In 2018, there were 22.692 Indonesian women dead because of breast cancer. Until now, the main cause of breast cancer is still unknown. However, the possibility of recovery and survival rates can be increased through early detection. One of the most efficient ways of early detection is through mammography. Mammography produces images called mammograms. The main objective of this paper is to develop Computer Aided Diagnosis (CADx) system that can help radiologist determine breast cancer cases based on mammogram image. In this paper, a combination of the Gray-level Co-Occurrence matrix (GLCM) and Backpropagation Neural Network (BPNN) is used to classify normal-abnormal patient based on mammogram image. Using mammogram image provided by Mammography Imaging Analysis Society (MIAS), a test for the proposed method was concluded. The result was, accuracy 94.06%, Sensitivity 90.16% , and Specificity 95.57%.

Keywords: *Breast Cancer, Mammography, MIAS, GLCM, BPNN*

1   Introduction

According to the [1], in 2018, there are estimated 626.679 (23.9%) women died because of worldwide. From that number, it is estimated that 22.692 are Indonesian. That is 32.5% of total women died because of cancer in Indonesia. American cancer society on their website said that the main causes of breast cancer are still unknown [2]. However, there are several ways that can be done to reduce the risk of breast cancer, such as maintaining weight, regular physical

activity, reduce or even avoid alcohol, breastfeeding [3]. Besides unhealthy lifestyle, breast cancer can also be caused by menstruation in younger age, menopause in the older age, late marriage, contraceptive drug, and hormone. In addition to a healthy lifestyle, early detection through routine checks is one of the things that can be done to prevent breast cancer. Early detection through routine examination can also improve recovery rates and survival rates. According to [4], the most effective and reliable method for detecting breast cancer in the early stages is mammography.

Mammography is done by illuminating the breast with X-ray rays. When the breast tissue is exposed to X-ray, breast tissue will absorb X-ray rays. Breast tissue and cancer cells have different signal outputs. The mammography process produces an image called a mammogram. However, mammograms have a high variability in breast masses appearance [5]. In some cases, abnormalities in the breast are also obscured by the structure of the breast tissue [6]. This can lead to biopsies that are not needed, even worse, missed malignant masses. This can cause the death of the patient. Furthermore, radiologist efficiency is closely related to experience and workload [7]. One solution that can be done to prevent this problem is Computer Aided Diagnosis (CADx). The CADx system is a set of automatic or semi-automatic tools created to help radiologists detect and classify breast abnormalities [8]. In recent years, CADx has been applied to help radiologists in detecting breast cancer [9].

The main objective of this paper is to develop a CADx systems to help radiologist classify breast cancer based on mammogram images. Mammogram images for cancer or abnormal cases have central coordinates of cancer and cancer radius. Based on that, the Region of Interest (ROI) will be generated. This is the first step of preprocessing. After ROI is obtained, ROI image will be converted into grayscale. Then, histogram equalization is performed to sharpen the contrast. After that, Gray-level Co-occurrence Matrices (GLCM) method is used to extract features from ROI. GLCM features used are Contrast, Dissimilarity, Homogeneity, ASM, and Energy. Last, Backpropagation Neural Network (BPNN) is used to identify normal-abnormal in mammograms. This research was conducted using Mammography Imaging Analysis Society (MIAS) dataset.

The rest of the paper is divided into, Section 2 describes the related works, Section 3 describes materials and methodology, Section 4 described the proposed method, Section 5 describes the results obtained, analysis and discussion, Section 6 describes conclusions and future works.

2   Related Works

Several studies to develop CADx system has been done in the past. A combination of Local Binary Pattern (LBP) and Support Vector Machine (SVM) is used in [10]. Otsu method is used in preprocessing step to remove the background. After that, LBP is used to compute feature vectors. 3x3 square

neighborhood centered at the given pixel is applied as LBP operator. Finally, SVM is used to classify normal-abnormal mammogram in Digital Database for Screening Mammography (DDSM) and MIAS dataset.

Another research done by [11] used GLCM to extract features from mammogram image. In the preprocessing step, mammogram images are cropped into ROI. GLCM is used to extract four features from ROI, which are ASM, Correlation, Sum Entropy and Sum Variance. After that, Pratiwi et. al. used Radial Basis Function Neural Network (RBFNN) to classify mammogram into normal-abnormal and benign-malignant cases. MIAS dataset is used to test out the proposed system.

In 2015, Setiawan and his team [12] developed the CADx system by combining Laws' texture energy measures (LAWS) and Artificial Neural Network (ANN). In their research, they used MIAS dataset. Their research is divided into three stages. The first step is cropping ROI from mammogram images. Then, LAWS is used to extract feature from mammogram images. Last, ANN is used to classify mammogram image into normal-abnormal class. In their testing, they compared LAWS-ANN with GLCM-ANN. Feature extracted using GLCM are ASM, Correlation, Sum of Variance and Difference Entropy.

A combination of Gabor wavelet and PCA with SVM is used by [13]. The Gabor wavelets are used to filtered mammogram images. Then, directional features are extracted at different orientation and frequencies. Dimensions of filtered and unfiltered high dimensional data are reduced by using Principal Component Analysis (PCA). Finally, the data is classified into three classes, normal-benign-malignant, normal-abnormal, and benign-malignant using Proximal Support Vector Machines (PSVM). Mammogram images are obtained from MIAS dataset.

3   Materials and Methodology

3.1   Breast Cancer

Cancer is a disease of the cells [14]. New cells will be produced to help growth, replace worn-out tissue and heal injuries. Normally, cells multiply and die regularly [14]. When this process runs irregularly, blood or lymph becomes abnormal or causes a lump called a tumor.

There are two types of tumors, namely benign and malignant. Benign tumors occur when cancer cells are confined in one area and do not spread to other parts of the body. This condition is not a cancer. While malignant tumors occur when cancer cells spread through the bloodstream or lymphatic system. This condition is called cancer.

According to [2] and [15], healthy lifestyle such as maintaining an ideal body weight, regular physical activity, reducing or even avoid alcohol can prevent breast cancer. For postmenopausal women, every 5-kg/m2 increase in BMI (Body

Mass Index), increases the risk of breast cancer by about 12% [16]. According to [17] [18] [19], 10-g-per-day alcohol consumption can increase the risk of developing breast cancer by 7% to 10%. For mortality rate, early detection and treatment reduce breast cancer mortality by 39% from 1989 to 2015 in the United States [20]. One way of early detection of breast cancer is to use a mammogram [21].

Based on the description above, our paper will focus on discussing CADx systems to help radiologist classify breast cancer based on mammogram images. In our paper, there are two target classes, namely normal (mammogram without tumor cells) and abnormal (benign and malignant tumors).

3.2   Mammogram

Mammograms are low-dose x-rays of breast tissue [22]. Mammograms are produced in a process called mammography. By using a mammogram, a lump(s) that are too small and cannot be felt during physical examination can be seen. During a mammography, the breast will be pressed between two x-ray plates, which spread the breast tissue so that a clear picture can be taken. This process takes about 20 seconds. A mammography will be performed on both breasts.

The mammogram is composed of black areas and white areas. The black area on the mammogram describes normal fatty tissue. While the white area on the mammogram describes ducts and lobules.

3.3 MIAS Database

The MIAS database can be downloaded at http://peipa.essex.ac.uk/info/mias.html for research purposes. MIAS database contains 200micron pixel edge and clipped/padded mammography images so that every image is 1024 × 1024 pixels. The images were taken from a screen-film mammographic British national breast screening program. Each mammogram image has a background network (fatty, fatty-glandular and dense glandular) and a class of abnormality (well defined or circumscribed masses, calcification, other or ill-defined masses, spiculated masses, asymmetry, architectural distortion, and normal). In addition to the abnormal class, there is additional information such as the severity of the disorder (benign or malignant), the coordinate center of the abnormality and the radius of the abnormality. Coordinate 0,0 is in the lower left corner of the image. The mammogram image is at the center of the MIAS database images. In this study, normal mammogram images will be classified as normal class. While the other class of abnormality will be classified as abnormal class. The abnormal and normal classes are shown in Fig. 1 (a) and Fig. 1(b) respectively.

(a)   (b)
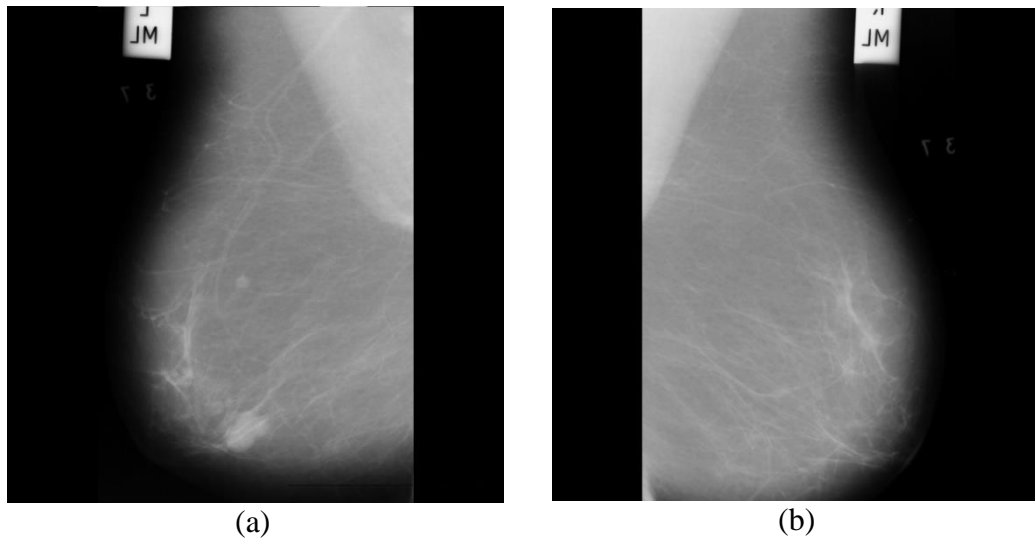
Fig. 1. MIAS Database Images. (a) Abnormal class (b) Normal class

3.4 Gray-level co-occurrence matrix (GLCM)

GLCM was developed by Haralic and his team [23]. The initial idea behind GLCM is to observe the gray level distribution between two pixels. This pixels is called the main pixel and the neighboring pixel. GLCM produces an output called the co-occurrence matrix or GLCM matrix. The GLCM computing stage begins by specifying one primary pixel and one neighboring pixel. Neighboring pixels must be in a certain distance and angle. This distance (D) and angle (Θ) is the GLCM parameter. GLCM algorithm is defined in Algorithm 1. The combination between D and Θ in GLCM is shown in Fig. 2. Fig. 3 shows the GLCM computing process.
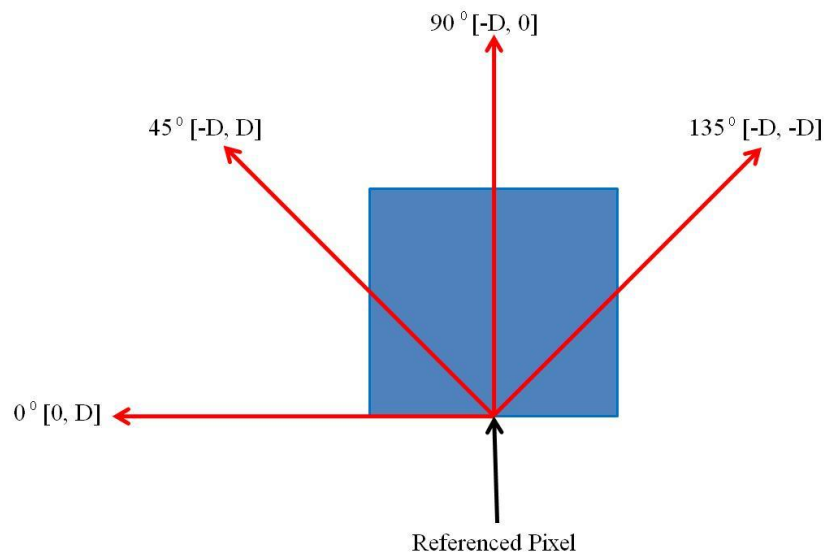
Fig. 2. $\boldsymbol{d}$ and $\boldsymbol{\Theta}$ in GLCM

Algorithm 1. GLCM Algorithm

1. Scan through the given image F and find the maximum gray-level value
2. Create a square matrix B with size $N*N$, where N is the gray-level from given image
3. Specify D and Θ
4. Count all pixel in image F that have value equals to $B[i][j]$ and have neighbor $B[k][l]$ in distance D and direction Θ
   Denote that i and j is the main pixel coordinate while k and l is the neighborhood pixel coordinate in distance D and direction Θ

	0	1	2	3
0	1	3	2	3
1	3	3	2	0
2	1	2	2	0
3	2	0	2	3

(a)

(b)	0	1	2	3
0	0	0	1	0
1	0	0	1	1
2	3	0	1	2
3	0	0	2	1

(c)	0	1	2	3
0	0	0	0	0
1	1	0	0	1
2	2	0	1	1
3	0	0	3	0

(d)	0	1	2	3
0	1	0	1	1
1	0	0	0	1
2	0	1	3	0
3	1	1	1	1

(e)	0	1	2	3
0	0	0	2	0
1	0	0	0	0
2	1	0	2	1
3	0	1	1	1

Fig. 3. GLCM example (a) 4 Gray levels of intensity values. Different GLCM matrix for set distance $D=1$ with four different angle combination is shown in (b) horizontal ($\boldsymbol{\Theta = 0^0}$) (c) right diagonal ($\boldsymbol{\Theta = 45^0}$) (d) vertical ($\boldsymbol{\Theta = 90^0}$) (e) left diagonal ($\boldsymbol{\Theta = 135^0}$)

Suppose there is image F with gray-level intensity shown in Fig. 3(a). Image F is an image with 4 gray levels of intensity values. Pixel with a value of 0 is choosen as the main pixel and pixel with a value of 2 is choosen as the neighboring pixel. Given $D = 1$ and $\Theta = 0^0$, there is 1 pixel in image F with a value of 0 that has a neighbor with a value of 2 on its right side. Therefore, cells (0,2) in Fig. 3(b) has a value of 1. Repeat this process for all cells in Fig. 3(b) to create GLCM Matrix for $D = 1$ and $\Theta = 0^0$. Using this method, GLCM Matrix with given $D=1$ and $\Theta = 45^0$ is created (shown in Fig. 3(c)), GLCM Matrix with given $D=1$ and $\Theta = 90^0$ is created (shown in Fig. 3(d)), and GLCM Matrix with given $D=1$ and $\Theta = 135^0$ is also created (shown in Fig. 3(d)).

After the GLCM matrix for all angles obtained, five features of each GLCM matrix will be extracted. The features used can be seen in Table 1. With regard to $\Theta = (0^0, 45^0, 90^0, 135^0)$, each features will have four value. Therefore, each image will have 20 features.

Table 1. Feature Descriptor GLCM

Feature descriptor	Name	Computation	
FD$_1$	Contrast	$\sum_{i,j=0}^{levels-1} P_{i,j}(i-j)^2$	(1)
FD$_2$	Dissimilarity	$\sum_{i,j=0}^{levels-1} P_{i,j}|i-j|$	(2)
FD$_3$	Homogeneity	$\sum_{i,j=0}^{levels-1} \dfrac{P_{i,j}}{1+(i-j)^2}$	(3)
FD$_4$	ASM	$\sum_{i,j=0}^{levels-1} P_{i,j}$	(4)
FD$_5$	Energy	$\sqrt{\sum_{i,j=0}^{levels-1} P_{i,j}|i-j|}$	(5)

3.5 Back Propagation Neural Network (BPNN)

BPNN is one example algorithm in artificial neural network field. The BPNN algorithm is defined in Algorithm 2 [24]:

Algorithm 2. BPNN Algorithm

1   Initialize random weights for each synapses in the neural network
2   Repeat for all hidden layers
3   For all sample training X do:
   3.1   Forward propagation for every X
   3.2   Backward propagation for each X
4   If the minimum error or maximum epoch has not been met, go back to step 2.
   4.1   Forward Propagation
         Calculate the output for each training sample X bypassing X through neurons in the network.
   4.2   Backward Propagation
         Calculate error in each output and hidden layer using Eq. (6) and Eq. (7)

$$\sigma_k = O_k(1-O_k)(t_k-O_k) \tag{6}$$

$$\delta_h = O_h(1-O_h)\sum_k w_{kh}\delta_k \tag{7}$$

   While the weight in each neuron will be updated with the Eq. (8)

$$w_{ji} = w_{ji} + \Delta w_{ji} \tag{8}$$

   which Δw_{ji} is defined as Eq. (9)

$$\Delta w_{ji} = \eta \delta_j X_{ij} \tag{9}$$

   η is the learning rate.

4   Proposed Method

4.1 Preprocessing

The first stage of preprocessing is cropping ROI. To crop the ROI, first, locate the coordinate center of the abnormality using the coordinate center information of the abnormality provided by MIAS. After that, using radius information, a circle around the center of the coordinate abnormality is created. By using the outer coordinate of the circle, made a square. Fig. 4 shows the process of cropping ROI. For normal class images, coordinate 512, 512 for x and y-axis respectively has been chosen. Using radius 128, a 256x256 ROI is taken.

After the ROI image created, the grayscale operation will be conducted. Due to contrast, usually, the quality of the original image is not very good. Therefore, improving the quality of the original image is necessary. Histogram equalization is used to sharpen the contrast between breast tissue and the background. Histogram equalization is a nonlinear redistribution of the image pixels' value [25]. Histogram equalization is done using Eq. (10)

$$\sum_{j=0}^{k} \frac{n_j}{n} * k \tag{10}$$

k is the maximum gray level value, is the gray level value of pixel j and n is image size.
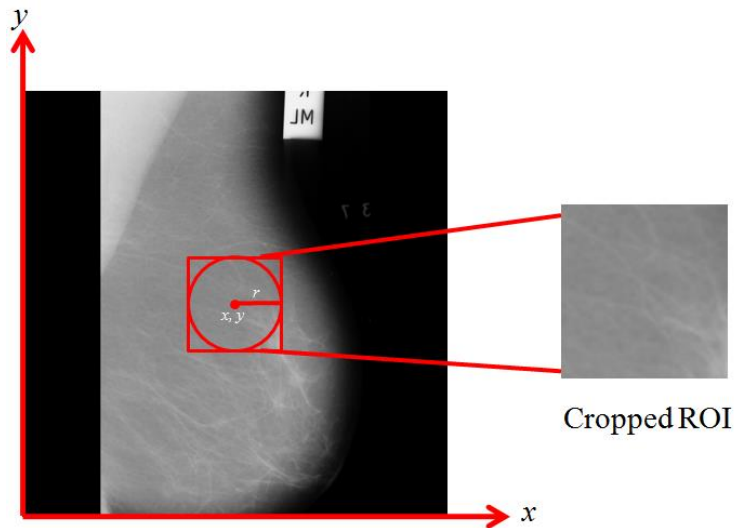
Fig. 4. Cropping ROI from mammographic image

(a)   (b)   (c)
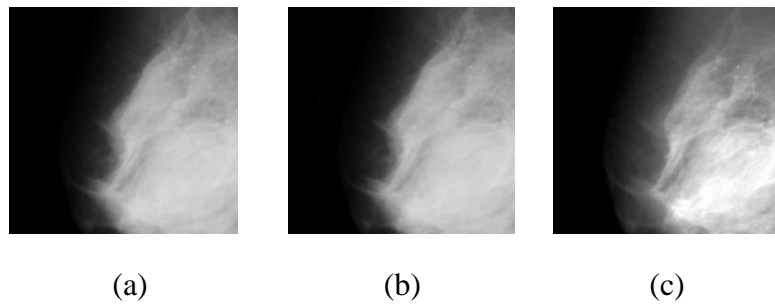
Fig. 5. Preprocessing results. (a) Original ROI, (b) Grayscale ROI, (c) Histogram Equalization ROI
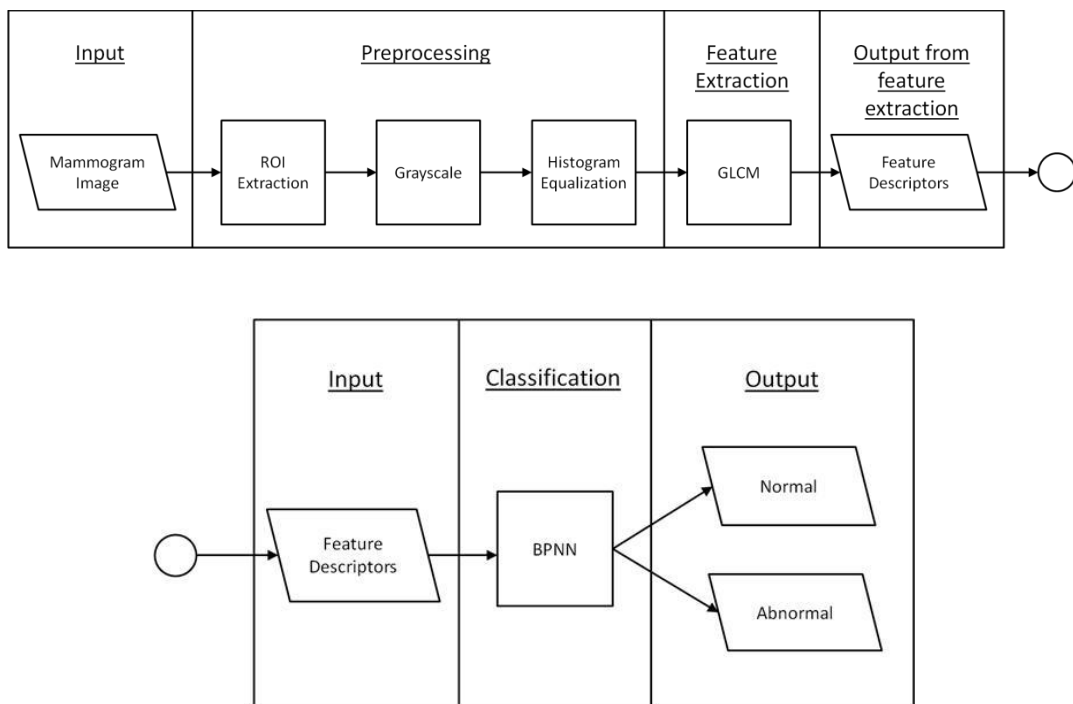
Fig. 6. GLCM-BPNN Architecture

Fig. 5 shows the preprocessing result, Fig. 5 (a) is the original image, Fig. 5 (b) is the grayscale image, Fig. 5 (c) is the histogram equalization image.

Due to $\Theta = (0^0,\ 45^0,\ 90^0, 135^0)$, each feature descriptor (FD) shown in Table 1 has four value. Max function in Eq. (11) is used to choose the representative value for every feature in each image. is the number of Feature Descriptor and is the number of images.

$$FD_{ij} = \ max(FD_i(\Theta = 0^0), FD_i(\Theta = 45^0), FD_i(\Theta = 90^0), FD_i(\Theta = 135^0)) \quad (11)$$

The architecture of the proposed method is shown in Fig. 6. The workflow of the GLCM-BPNN algorithm is as follows:

1. Take a mammogram image as input.
2. The next step is preprocessing. Preprocessig consist of three steps as follows:
    2.1. ROI Extraction
        The mammography images were cropped using the cancer coordinate center and radius information provided by MIAS. For normal classes, the 512,512 point is selected as the coordinate center. Then by using a 128-pixel radius, the ROI will be created.
    2.2. Greyscale Operation
    2.3. Histogram Equalization to sharpen the image
3. After pre-processing is complete, the next step is feature extraction using GLCM. Each mammogram image has 5 features as shown in Table 1. Since the number of θ used are four $(0^0, 45^0, 90^0, 135^0)$, each feature has 4 values. To find the most representative value, the maximal rule of Eq. (11) is used.
4. Due to some feature descriptor value is bigger than 2 million, while the target output is 0 for Normal class and 1 for Abnormal class, normalization is used to equalize the feature descriptor (input in BPNN) and target class in BPNN.
5. Next is BPNN training. To train BPNN, 100 mammogram images are selected at random. 50 normal classes, 50 abnormal classes. Unselected data is used as test data. The number of the epoch, number of neuron in the hidden layer will be explained in Section 5. In the output layer, there are two neurons.
6. Neuron with the value of 1 is abnormal class and neuron with the value of 0 is the normal class.
7. Finally, GLCM-BPNN will be tested using accuracy, sensitivity, and specificity testing.
    7.1. Accuracy

    Accuracy testing is done to measure the overall system capability. It is important to measure the ability of a system that has been made [26]. The formula for accuracy can be seen in Eq. (12)

    $$Accuration = \frac{TP + TN}{TP + TN + FP + FN} x\ 100\% \tag{12}$$

    7.2. Sensitivity
        Sensitivity testing is done to measure the ability of the system to accurately identify the desired classes. The formula for sensitivity can be seen in Eq. (13)

    $$Sensitivity = \frac{TP}{TP + FN} x\ 100\% \tag{13}$$

    7.3. Specificity

Sensitivity testing is done to measure the ability of the system to accurately identify unwanted classes. The formula for specificity can be seen in Eq. (14)

$$Specificity = \frac{TP}{TN + FP} x\ 100\% \tag{14}$$

TP, TN, FP, and *FN* are true positives, true negatives, false positives and false negatives respectively.

- *TP*: The system predicts input as an abnormal class, so does MIAS.
- *TN*: The system predicts input as a normal class, so does MIAS.
- *FP*: The system predicts input as an abnormal class, but MIAS considers input as a normal class.
- *FN*: The system predicts input as a normal class, but MIAS considers input as an abnormal class.

5   Results, Analysis, and Discussions

Due to the incomplete of data, mammogram image number 59, 216, 233 and 245 are removed from the dataset.

The ability of BPNN to complete a task is influenced by the learning process. Parameters that affect the learning process include the number of the epoch and the number of neurons. Therefore, testing is needed to determine the best number of epoch and number of neurons. The test results of the epoch number can be seen in Fig. 7. the x-axis represents the number of epochs and y-axis represent an error. The detailed result can be seen in Table 2. In this test, the number of neurons used is 10. Based on test results, can be seen if the error value decreased gradually until epoch 50000. Because the error decreasing from 20000 epochs to 25000 epochs is only 0.000066385 (from 0.040131 to 0.04064) and keep getting smaller, 20000 epoch has been selected.
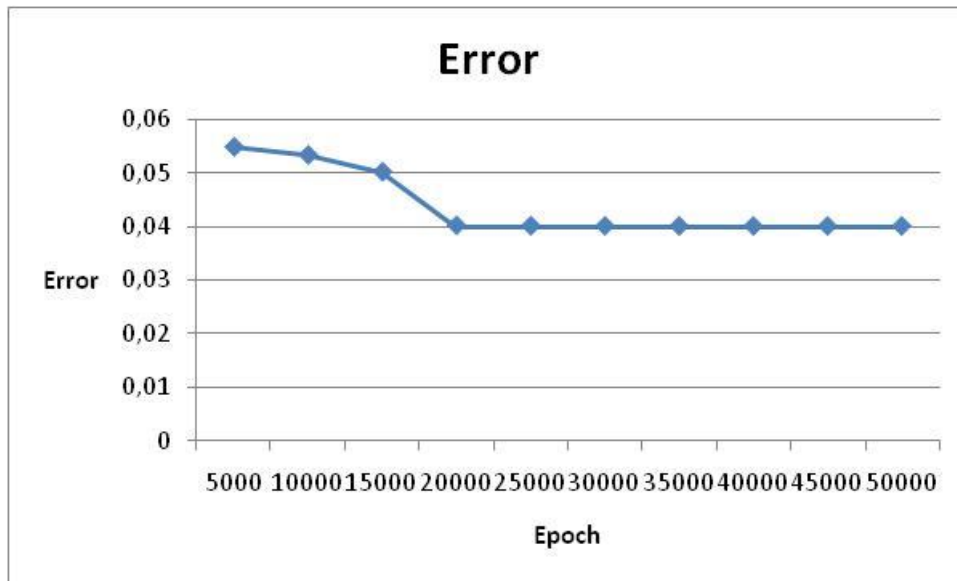
Fig. 7. Epoch test results

Table 2. Epoch test details	
Epoch	Error
5000	0.05481
10000	0.053313
15000	0.050165
20000	0.040131
25000	0.040064
30000	0.040042
35000	0.040031
40000	0.040024
45000	0.04002
50000	0.040017

Table 3. Neuron test details	
Neuron	Error
2	0.062604
3	0.058063
4	0.058395
5	0.058506
6	0.068862
7	0.058753
8	0.040473
9	0.059117
10	0.053313
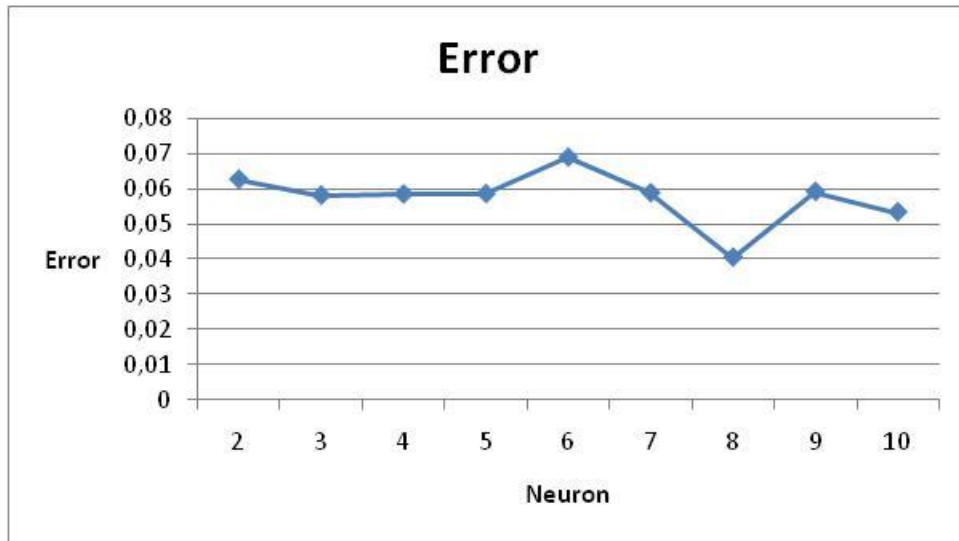
Fig. 8. Neuron testing result

As for testing the number of neurons, the number of epoch used is 10000. The results of neuron testing can be seen in Fig. 8. the x-axis represents the number of neurons and the y-axis represents the error value. The detailed result can be seen in Table 3. Based on Fig. 8, can be seen if the error value varies. Based on test results, 8 neurons were selected because they have the smallest error value (0.40473).

After the epoch number and the number of neurons obtained, then training on the BPNN network. The first stage of training is ROI Extraction from mammogram images. After that, ROI contrast will be sharpen using histogram equalization. Then, GLCM will be performed to get the feature from the image. The feature extracted from GLCM can be seen in Table 1. Finally, the GLCM feature will be used as input on the Backpropagation input layer.

Table 4. Detailed Result

Method reference	Techniques	Classification performance (normal-abnormal)
[3]	GLCM-SVM	Accuracy = 63.03% Specificity = 89.01%
[10]	LBP, SVM	Accuracy = 84%
[11]	GLCM, RBFNN	Accuracy = 93.98% Sensitivity = 97.22%, Specificity = 91.49%,
[12]	LAWS, ANN	Accuracy = 93.90%, Sensitivity = 100%, Specificity = 91%
[13]	Gabor wavelet and PCA, SVM	Sensitivity = 97.56%, Specificity = 60.86%

Proposed Method	GLCM-BPNN	Accuracy = 94.06%, Sensitivity = 90.16%, Specificity = 95.57%

Finally, a comparative analysis between the proposed method with other existing studies is shown in Table 4. According to Table 4, the proposed method have better performance than other studies with respect to different performance measures. In terms of Accuracy and Specificity, the proposed method outperformed other studies with Accuracy of 94.6% and Specificity 95.75%. However, in term of Sensitivity, the proposed method still loses when compared to GLCM-RBFNN [9] and LAWS-ANN [10]. Therefore, to increase its performance, the proposed method requires more feature extracted and data, so it can perform better.

6   Conclusion

In our paper, breast cancer classification methods are classified using a combination of GLCM and BPNN methods. By using GLCM, BPNN does not need to learn all the pixels in the ROI. By reducing the number of input neurons from about 256x256 to 5, the learning time required by BPNN could be drastically reduced. To test the proposed method, 20000 epoch and 8 hidden neurons were selected. Using GLCM-BPNN, a Specificity 95.57%, sensitivity 90.16% and Accuracy of 94.06% were obtained for normal-abnormal MIAS databases.

For future work, GLCM-BPNN will be applied to classify benign-malignant classification as well. In our paper, ROI was generated manually using information provided by MIAS databases. For further research, a method that can extract ROI automatically may be used.

References

[1]   Gco.iarc.fr, "Cancer today," 2018. [Online]. Available: http://gco.iarc.fr/today/online-analysis-pie?v=2018&mode=cancer&mode_population=continents&population=900 &populations=900&key=total&sex=2&cancer=39&type=1&statistic=5&pr evalence=0&population_group=0&ages_group%5B%5D=0&ages_group% 5B%5D=17&nb_items=7&group_. [Accessed 12 December 2018].

[2]   ACS, "American Cancer Society | Information and Resources about for Cancer: Breast, Colon, Lung, Prostate, Skin," 2018. [Online]. Available: https://www.cancer.org/. [Accessed 22 August 2018].

[3]   S. J. A. Sarosa, F. Utaminingrum and F. A. Bachtiar, "Mammogram Breast Cancer Classification Using Gray-Level Co-Occurrence Matrix and Support

Vector Machine," in *2018 International Conference on Sustainable Information Engineering and Technology (SIET)*, Malang, 2018.

[4] L. Tabar and P. Dean, "Mammography and breast cancer: the new era," *Int. J. Gynecol. Obstet 82,* pp. 319-326, 2003.

[5] J. Ball and L. Bruce, "Digital Mammographic Computer Aided Diagnosis (CAD) using Adaptive Level Set Segmentation," in *2007 29th Annual International Conference of the IEEE Engineering in Medicine and Biology Society*, 2007.

[6] B. Verma, P. McLeod and A. Klevansky, "Classification of benign and malignant patterns in digital mammograms for the diagnosis of breast cancer," *Expert Systems with Applications 37,* p. 3344–3351, 2010.

[7] J. G. Elmore, S. L. Jackson, L. Abraham, D. L. Miglioretti, P. A. Carney, B. M. Geller, B. C. Yankaskas, K. Kerlikowske, T. R. Onega, D. Rosenberg and e. al, "Variability in interpretive performance at screening mammography and radiologists' characteristics associated with accuracy," *Radiology,* pp. 641-651, 2009.

[8] T. Freer and M. J. Ulissey, "Screening mammography with computer-aided detection: Prospective study of 12,860 patients in a community breast center," *Radiology 220,* pp. 781-786, 2001.

[9] V. Changizi, M. Giti and A. Kheramand, "Application of computed aided detection in breast masses diagnosis," *Indian journal of cancer, vol 45, no. 4,* 2008.

[10] P. Král and L. Lenc, "LBP features for breast cancer detection," *International Conference on Image Processing (ICIP),* pp. 2643-2647, 2016.

[11] M. Pratiwi, Alexander, J. Harefa and S. Nanda, "Mammograms Classification using Gray-level Co-occurrence Matrix and Radial Basis Function Neural Network," in *Procedia Computer Science 59*, 2015.

[12] A. S. Setiawan, Elysia, J. Wesley and Y. Purnama, "Mammogram Classification using Law's Texture Energy Measure and Neural Networks," in *Procedia Computer Science 59*, 2015.

[13] I. Buciu and A. Gacsadi, "Directional features for automatic tumor classification of mammogram images," *Biomed. Signal Process. Control 6,* pp. 370-378, 2011.

[14] C. Groove and P. Marchant, Understanding Breast Cancer: A guide for people with cancer, their families and friends, Sydney: Cancer Council Australia, 2016.

[15] A. G. Colditz and K. Bohlke, "Priorities for the Primary Prevention of Breast Cancer," *A Cancer Journal for Clinicians,* pp. 186-194, 2014.

[16] A. Renehan, M. Tyson, M. Egger, R. Heller and M. Zwahlen, "Body-mass index and incidence of cancer: a systematic review and meta-analysis of

prospective observational studies," *The Lancet, vol. 371, no. 9612,* pp. 569-578, 2008.

[17] W. Chen, B. Rosner, S. Hankinson, G. Colditz and W. Willett, "Moderate Alcohol Consumption During Adult Life, Drinking Patterns, and Breast Cancer Risk," *JAMA, vol. 306, no. 17,* pp. 1884-1890, 2011.

[18] S. Smith-Warner, D. Spiegelman and S. e. a. Yaun, "Alcohol and breast cancer in women: a pooled analysis of cohort studies.," *Southern Medical Journal, vol. 91, no. 7,* pp. 535-540, 1998.

[19] N. Hamajima, K. Hirose and K. Tajima, "Alcohol, tobacco and breast cancer – collaborative reanalysis of individual data from 53 epidemiological studies, including 58 515 women with breast cancer and 95 067 women without the disease," *British Journal of Cancer, vol. 87, no. 11,* pp. 1234-1245, 2002.

[20] R. L. Siegel, K. D. Miller and A. Jemal, "Cancer Statistic, 2018," *CA Cancer J Clin, Volume 68,* pp. 7-30, 2018.

[21] F. K. Nezhadian and S. Rashidi, "Breast cancer detection without removal pectoral muscle by extraction turn counts feature," *Artificial Intelligence and Signal Processing (AISP),* pp. 6-10, 2017.

[22] C. C. Australia, Understanding Breast Cancer : A guide for people with cancer, their families and friends, Sydney, 2016.

[23] R. M. Haralic, K. Shanmugam and I. H. Dinstein, "Textural Features For Image Classification," vol. 3, no. 6, 1973.

[24] S. Chauhan, V. Goel and S. Dhingra, "Pattern recognition system using MLP neural Network," *Pattern Recognition, 4(9),* pp. 43-46, 2012.

[25] W. Zhihong and X. Xiaohong, "Study in Histogram Equalization," *International Symposium on Intelligence Information Processing and Trusted Computing,* pp. 177-179, 2011.

[26] F. Utaminingrum, Y. A. Sari and R. P. Primaswara, "Image Processing For Rapidly Eye Detection Based On Robust Haar Sliding Window," vol. 7, no. 2, 2017.